MODELING AND SIMULATION OF REFORMER AUTO-THERMAL REACTOR IN AMMONIA UNIT

Kayvan Khorsand[*], Khadijeh Dehghan

*Research Institute of Petroleum Industry (RIPI),Tehran, Iran,
P.O. Box: 18745-4163, E-mail: khorsandk@ripi.ir*

Abstract

In this paper, reformer auto-thermal reactor, which is the secondary reformer reactor in ammonia unit, has been modeled and simulated. The secondary reformer reactor is located after the primary one and consists of a combustion chamber and a catalytic bed. For simulation of this reactor, combustion chamber (flame area) has been modeled assuming that the feed and excess inlet air to the reactor are fully mixed along the flame. Modeling of flame area yields flame temperature and concentration of reactor components and product, which have been used in modeling of catalytic bed. Finally, the results of this simulation have been compared with the industrial data taken from the existing ammonia unit in Khorasan Petrochemical Complex, which show a relatively good compatibility.

Key words: Auto-thermal, Reformer, Modeling, Simulation, Ammonia

1. Introduction

Secondary reformer reactor plays an important role in ammonia production units. This reactor, which is placed after the primary reformer, fulfils the process of methane to hydrogen conversion. In addition it will generate the required nitrogen for the process and adjusts the optimum nitrogen to hydrogen ratio required for the ammonia synthesis reaction. To achieve the optimum ratio, the synthesis gas to nitrogen ratio shall come close enough to the required value in the beginning of the process cycle, which is fulfilled by the secondary reformer. Excess air in accompany with fuel is entered to flame area to yield the desired amount for the output of the reactor. The secondary reformer is important in the production of ammonia as it adjusts the N_2 to H_2 ratio and controls mixing of these two fundamental components in the reactor. In fact, operation of the secondary reformer reactor depends upon incoming air mixture and gas feed which is the output of the primary reformer.
Secondary reformer substantial reactions are as below:

$$CH_4 + H_2O \Leftrightarrow CO + 3H_2 \tag{1}$$
$$CO + H_2O \Leftrightarrow CO_2 + H_2 \tag{2}$$
$$H_2 + 0.5O_2 \Rightarrow H_2O \tag{3}$$
$$2CO + O_2 \Rightarrow 2CO_2 \tag{4}$$
$$2CH_4 + O_2 \Rightarrow 2CO + 4H_2 \tag{5}$$

Reactions (1) and (2) are for catalytic bed area and reactions (3-5) are related to combustion area. The substantial reactions conducted in combustion area of the secondary reformer reactor includes burning of hydrogen as the incoming gas from primary reformer includes a lot of hydrogen and hence its burning kinetics has to be incorporated to forecast the gas components concentrations and temperatures.
The schematic diagram of the mentioned areas and the components abbreviations has been depicted in figure (1).
The following assumptions have been taken in to account for modeling of the reactor:

a) The system is assumed to be unidirectional in the direction of fluid movement.
b) As the fluid speed in the reactor is very high, the effects of mass penetration and temperature have been ignored. Also the fluid is not subject to radial diffusion.
c) In studies related to the specifications of the gas mixture, relations of ideal fluid and in some cases ideal gas have been incorporated.
d) There is no oxygen after the combustion area.
e) The reactor is adiabatic from thermal point of view.
f) It is assumed that the feed and the incoming excess air to the reactor are fully mixed along the flame.
g) The reactions in combustion area are assumed to be under equilibrium

2.1 Modeling of flame area

Flame area in secondary reformer has an important role in adjustment of N_2 to H_2 ratio. The amount of inlet air to the reactor should assure complete combustion of O_2 before its arrival to the catalytic bed and yield an optimum ratio for N_2 and H_2+CO for synthesis reactor. In literature this optimum value is 2-3.5 [1,2,5]. By modeling of flame area it will be possible to precisely estimate the temperature changes and gas components by changing the concentration of inlet feed and air to the reactor. Karim and Metwally (1980) [1] have investigated the kinetic behavior of steam-methane homogenous mixture in temperature range of 1400 – 3000 K, pressure of 0.5 – 1 atm. and steam to methane ratio of 1-5. They showed that in the mentioned operating conditions and the amount of steam to methane ratio of more than 1, carbonization would not occur considerably and hence the nature of the reaction is homogenous. This result has been incorporated in the assumptions of the current modeling.

The important point in reforming process is that components concentrations are less sensitive to process pressure. For instance, pressure impact on product concentration is very low in a wide range of residence times say 1-1000 second. On the other hand, steam to carbon ratio has a high impact on the products concentrations such as CO, H_2 and CO_2 [1].
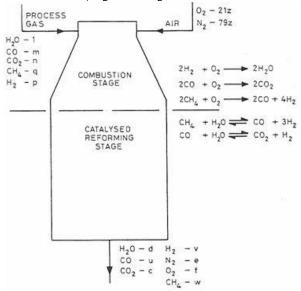

Fig. (1) – Schematics of the main area of the secondary reformer reactor

2.2. Heat and Mass balance in flame area

Considering the assumptions made for modeling of the flame area, reactions have been considered to be in equilibrium [2,5]. This assumption seems reasonable, as the goal of the modeling is to derive flame area temperature, concentration of different components at the end of combustion and the optimum ratio of input air to feed from primary reformer to secondary one.

Assuming $l+m+n+p+q=100$ mol for input feed to the secondary reformer and considering item "d" of the modeling assumptions, if x_1, x_2 and x_3 are assumed as molar consumptions of oxygen in reactions (3), (4) and (5) respectively, then applying of molar balance equation of oxygen

around the reactor yields $x_3 = 21z - x_1 - x_2$ and considering item "g" of the modeling assumptions and equilibrium relations for all components, x_1 and x_2 can be derived.

As illustrated in Fig (1), the required relations for molar balance of the main components are as follow:

N_2 Balance:
$$e = 79z \tag{6}$$

H_2 Balance:
$$l + 2q + p = d + v + 2w \tag{7}$$

O_2 Balance:
$$21z + n + \frac{m+l}{2} = \frac{d+u}{2} + c + f \tag{8}$$

C Balance:
$$m + n + q = u + w + c \tag{9}$$

Simultaneous incorporate of equilateral relations for reactions (3) and (4) yields:

$$\frac{(l + 2x_1)[m - 2x_2 + 2(21z - x_1 - x_2)]}{[p - 2x_1 + 4(21z - x_1 - x_2)](n + 2x_2)} = \left(K_3 / K_4\right)^{0.5} \tag{10}$$

According to relations given in [2], equilibrium constants of reactions (3) and (4) are related to temperature based on the following equation:

$$Log\ (K_3/K_4)^{0.5} = 0.755\text{-}850/T_c \tag{11}$$

Similarly for reactions (4) and (5), we have:

$$DK = \frac{[p - 2x_1 + 4(21z - x_1 - x_2)]^2 [m - 2x_2 + 2(21z - x_1 - x_2)]^2 P^2}{[q - 2(21z - x_1 - x_2)](n + 2x_2)(100 + 163z - 4x_1 - 4x_2)^2} - (K_5 / K_4)^{0.5} \tag{12}$$

In which the equilibrium constants have the following relation with temperature:

$$Log\ (K_5/K_4)^{0.5} = -2.945\text{-}6692.5/T_c \tag{13}$$

x_1 will have an integer value when DK=0.

After derivation of x_1, x_2, x_3 and z, concentration of reaction components after combustion will be obtained by means of molar balance.

For calculation of sensible heat changes the following relation will be used:

$$HS \Big|_{T_r}^{T_p} = \sum_{i=1}^{5} \int_{T_o}^{T_p} (p_i C_{pi}) dT - \sum_{i=1}^{5} \int_{T_o}^{T_r} (r_i C_{pi}) dT \tag{14}$$

Total heat of reactions (3), (4) and (5) is obtained by the following relation:

$$HR_{3,4,5} = \sum_{i=1}^{4} p_i (HF)_{T_{c,i}} - \sum_{i=1}^{4} r_i (HF)_{T_{c,i}} \tag{15}$$

Target function will be based on energy balance of the combustion chamber. If the temperature of the combustion area, T_c, is calculated correctly, DHC will be zero:

$$DHC = 10^3 HR_{3,4,5} - HS \Big|_{T_r}^{T_c} \tag{16}$$

Simultaneous solving of heat and mass balance equations, will yield the flame temperature and reactor components concentrations at the end of the flame area which will be considered as input data to catalytic bed area.

3. Modeling of Catalytic Bed

The mathematical model has been derived based on the models offered for the secondary reformer in [2,3,4,5]. The kinetics for the reforming reaction of methane with Alumina based nickel catalysts is according to those given in [4].
Considering the 5 important reactions conducted in combustion chamber and reforming catalytic bed and also the heat transfer restrictions stating that there is not any transfer of heat in the reactor walls and the heat transfer related to partial combustion and reforming will be only in combustion chamber, the secondary reformer reactor will have a one dimensional heterogeneous and adiabatic model [2,3,4]. It is of course important to consider the effect of local hot spot on activity and longevity of the catalyst.

3.1 Heat and Mass Balance in Catalytic Bed

As the model used for the catalytic reactions of the secondary reformer reactor is one dimensional and heterogeneous, considering reactions (1) and (2), mass balance equation for component 'i' along the reactor will be as follows:

$$\frac{\partial n_i}{\partial \ell} = \sum_{k=1}^{2} \xi_{i,k} \eta_k r_k (1-\varepsilon) A \qquad (17)$$

Component i can be CO, H_2, CH_4, H_2O and CO_2. For nitrogen, argon and inactive components, the simple relation of $\sum_{i=1} n_i = n_T$ will be used. η_k Is the catalyst effectiveness factor, r_k is the rate of reaction k, A is the reactor cross section area, $\xi_{i,k}$ is the stoichiometry coefficient of component i in reaction k and ε is the porosity of catalytic bed.
Considering that the resulted heat from heat transfer between gas and catalyst surface is equal to the reactions heat in steady state, the heat balance equation can be written as below:

$$\sum_{k=1}^{2} \Delta H_k \eta_k r_k (1-\varepsilon) = \frac{6(1-\varepsilon)h(T_g - T_s)}{D_s} \qquad (18)$$

Heat transfer coefficient in catalyst surface will be derived using the below relation [5]:

$$NU = 0.4 \mathrm{Re}_p^{0.64} \, pr^{\frac{1}{3}} \qquad (19)$$

So the heat balance equation for the gas phase along axial direction will be as follows:

$$F_g C_{p_g} \rho_g \frac{\partial T_g}{\partial \ell} = \sum_{k=1}^{2} \Delta H_k \eta_k r_k (1-\varepsilon) A \qquad (20)$$

In which F_g is the molar flow rate of the gas phase.

Using the mentioned equations it will be possible to forecast the molar distribution of each component, gas temperature and catalyst surface temperature along the bed. As the simulation of the reactor is done in steady state, partial differentials will be converted to complete differentials.

3.2. Momentum Balance in Catalytic Bed

Applying Ergun relation for catalytic bed, it will be possible to calculate the pressure drop as be below [8]:

$$\frac{-dP}{d\ell} = \frac{G}{\rho g_c D_p}(\frac{1-\varepsilon}{\varepsilon^3})\left[\frac{150(1-\varepsilon)\mu}{D_p} + 1.75G\right]$$ (21)

μ - the average viscosity of gas mixture in the bed,

D_p - the diameter of catalyst particles,

ρ - the density of gas mixture inside bed and

G - the mass flux of the gas inside bed.

Relations of all the other physical parameters with temperature, pressure and concentrations are according to reference [7].

4. Results and Discussion

The operating conditions as well as concentration of input components to the reactor adopted from documents and PFD of Khorasan Petrochemical Complex Ammonia Unit have been given in Tables (1) and (2). The output values of the reactor in both cases have been compared in Table (2).

Temperature distribution along the catalytic bed has been illustrated in Fig (2). As the industrial data along the reactor are not available, only the input temperature to the reactor, temperature of the combustion area and output temperature have been compared with the industrial data. According to the simulation results, temperature of the combustion chamber is 1242°C, which is quite compatible with the real value of 1247°C. Values of the components concentrations have been given in Table (2). As there is no industrial data available in this area, they are not comparable.

Considering the results obtained from modeling and the assumptions made for the combustion chamber, the main part of the model shows a good compatibility with the industrial unit. For better and precise forecast of this area behavior, the kinetic model of the combustion shall be also incorporated.
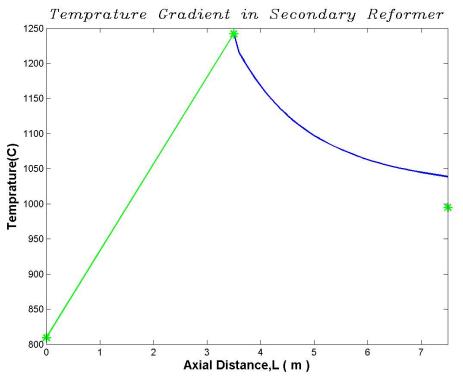

Fig (2): Distribution of Temperature along the Catalytic Bed

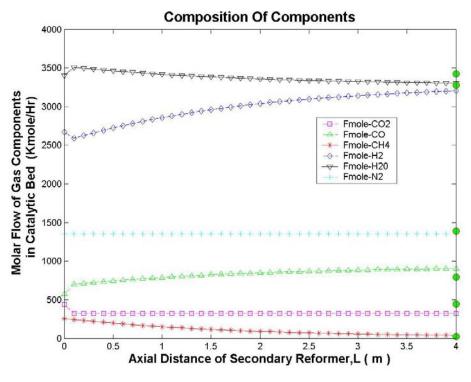**Composition Of Components**

Fig (3): Distribution of Components Concentrations along the Catalytic Bed

Distribution of components concentrations has been depicted in Fig (3). Concentration of the components in the outlet of the combustion chamber and input to the reactor catalytic bed has been given in table (2). Comparison has been only done in catalytic bed, as industrial data are not available for the other sections. Fig (4) illustrates the distribution of catalyst surface temperature along the catalytic bed. Fig (5) shows the pressure drop along the catalytic bed, which shows quite a good compatibility with the industrial reactor data.
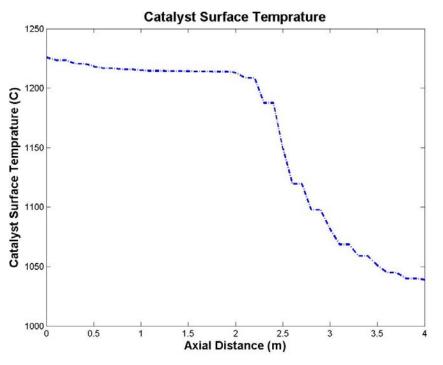
Catalyst Surface Temprature

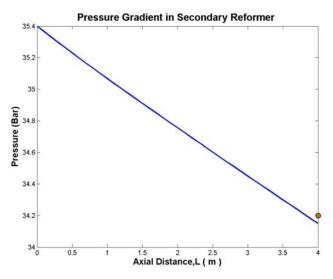Fig (4): Distribution of Catalyst Surface Temperature along the bed

Fig (5): Pressure Drop Variation along the Catalytic Bed

Table (1): Input Data of the Industrial Reactor [11]

Parameters	Input Feed to the Secondary Reformer (Output of the Primary Reformer)	Input Air to the Secondary Reformer
Temperature, ^{o}C	809.3	610
Pressure, bar	35.4	35.4
Molar Flow Rates of the Components, kmol/hr		
H_2	2699.4	0
N_2	18.9	1370.8
CH_4	498.5	0
Air+ Inert	0.2	16.5
CO	369.3	0
CO_2	397.3	0.5
O_2	0	368.7
H_2O	2884.6	175.6

Table (2): Output Data of the Industrial Unit and Simulation

Parameters	Output of the Secondary Reformer (Industrial Unit)	Output of the Combustion Area and Input to Catalytic Bed (Simulation)	Output of the Secondary Reformer (Simulation)
Temperature, ^{o}C	993.9	1242	1038.8
Pressure, bar	34.2	35.4	34.149
Molar Flow Rates of the Components, kmol/hr			
H_2	3426.5	2671.1	3200.1
N_2	1389.7	1389.7	1389.7
CH_4	26.2	253.05	36.657
Air+ Inert	16.7	16.7	16.7
CO	794	573.79	905.41
CO_2	445.5	438.26	323.04
O_2	0	0	0
H_2O	3302.7	3403.8	7896.9

References

[1]   Karim, G.A. and M.M. Metwally, Int. J. Hydrogen Energy, Vol. 5, 1980, pp 293-304.
[2]   Davies, J.; and Lihou, D. A.; Optimal Design of Methane Steam Reformer; Chemical and Process Engineering; April 1971; pp: 71-80.
[3]   De Groote, Ann M., and Gilbert F. Froment, Applied Catalysis A: General, Volume 138, Issue 2, 1996, Pages 245-264.
[4]   Xu, J. & Froment G.F.; Methane Steam Reforming: II. Diffusional Limitations and Reactor Simulation; AIChE Journal; 1989; Vol. 35; No.1.
[5]   Yu. Y.H.; Simulation of Secondary Reformer in Industrial Ammonia plant; Chemical Engineering and Technology; Vol.25 (3); 2002; pp: 307-314.
[6]   Froment, G.F.; and Bischoff, K.B.; Chemical Reactor Analysis and Design, 1990, John Wiley & Sons, 2 Ed.
[7]   Elashie S.S.E.H Elshishini; Modeling, Simulation and Optimization of Industrial Fixed Bed Catalytic Reactors; 1993.
[8]   Witt, P. M. and L. D. Schmidt, Journal of Catalysis, Vol. 163, Issue 2 , 1996 , Pages 465-475
[9]   Tsipouriari, V. A., Zhang, Z. and X. E. Verykios, Journal of Catalysis ,Volume 179, Issue 1, 1998, Pages 283-291.
[10]   Feasibility Study on Technology Transfer and Localization of Ammonia Production Unit, Research Institute of Petroleum Industries, 1380.
[11]   KHPC technical documents.
[12]   http://www.webbook.org.